Korean J. Chem. Eng., 40(7), 1725-1730 (2023)
DOI: 10.1007/s11814-023-1385-3

pISSN: 0256-1115
eISSN: 1975-7220

Guest distributions and dissociation enthalpy of fluorinated gas (CHF_3 or C_2F_6)+N_2 hydrates for hydrate-based gas separation

Gyeol Ko*,‡, Eunae Kim,‡, Dongyoung Lee*, and Yongwon Seo*,***,†**

*Department of Urban and Environmental Engineering, Ulsan National Institute of Science and Technology, Ulsan 44919, Korea
**Particulate Matter Research Center, Research Institute of Industrial Science & Technology, Jeollanam-do 57801, Korea
***Graduate School of Carbon Neutrality, Ulsan National Institute of Science and Technology, Ulsan 44919, Korea
(*Received 28 November 2022 • Revised 22 December 2022 • Accepted 23 December 2022*)

Abstract−Fluorinated gases (F-gases), such as CHF_3 and C_2F_6, which are used in the semiconductor industry and have considerable global warming potential, can be recovered after use through a gas hydrate-based separation method to prevent their release into the atmosphere. In this study, the guest distributions and dissociation enthalpy (ΔH_d) of F-gas (CHF_3 or C_2F_6)+N_2 hydrates with different F-gas concentrations (CHF_3: 20%, 80%, and 100% and C_2F_6: 20%, 60%, 80%, and 100%) were experimentally investigated using a powder X-ray diffractometer and a high-pressure micro-differential scanning calorimeter, respectively. At high N_2 concentrations in the feed gas, the occupancy of N_2 in the small (5^{12}) cages of the F-gas+N_2 hydrates increased significantly. As a result, the F-gas+N_2 hydrates exhibited reduced hydration numbers at high N_2 concentration. The ΔH_d values (in kJ/mol gas) of the F-gas (CHF_3 or C_2F_6)+N_2 hydrates decreased with increased N_2 concentration. The overall experimental results provide useful insights into the design and operation of gas hydrate-based F-gas separation processes.

Keywords: CHF_3, C_2F_6, Dissociation Enthalpy, Gas Separation, Cage Occupancy, Gas Hydrates

INTRODUCTION

Gas hydrates are crystalline inclusion compounds composed of guest molecules and hydrogen-bonded host water frameworks in high-pressure and low-temperature environments [1,2]. Water molecules of host lattices interact with guest molecules entrapped in hydrate cages by van der Waals forces [2]. The three major structures of gas hydrates, known as structure I (sI), structure II (sII), and structure H (sH), are mainly determined by the molecular size of guest molecules [2]. Gas hydrates have been widely studied for their potential applications in various energy and environmental fields, such as storage and transportation media for gaseous energy sources (CH_4 and H_2) [3-10], CO_2 capture and sequestration [7,8,11-31], and desalination [23,31-37]. In particular, hydrate-based gas separation has been investigated in various target gases, including CO_2 [7,8,11-17], light hydrocarbons [18-23], and fluorinated gases (F-gases) [24-31], as it has good potential for high-separation efficiency and eco-friendly operation.

In this sense, our previous studies examined hydrate-based F-gas separation for CHF_3 and C_2F_6 because CHF_3 and C_2F are widely used in the semiconductor industry due to their molecular stability and reusability, despite their high global warming potential [26-28]. Kim et al. studied the thermodynamic and structural properties of pure CHF_3 and C_2F_6 hydrates, including hydrate phase equilibria, structural identification, and cage-filling behavior of these F-gas hydrates [26]. They also demonstrated the feasibility of hydrate-based F-gas (CHF_3 or C_2F_6) separation by analyzing the gas hydrates formed at different feed gas concentrations of F-gases balanced with N_2 [27,28]. Furthermore, they examined the thermodynamic gas separation efficiency at a constant temperature condition (279.15 K for CHF_3+N_2 hydrates and 275.15 K for C_2F_6+N_2 hydrates), with an identical pressure driving force of ΔP=1.0 MPa. The results indicated that the CHF_3 (20%)+N_2 (80%) gas mixture can be concentrated to 90% CHF_3 after two steps of hydrate formation, whereas the C_2F_6 (20%)+N_2 (80%) gas mixture can be enriched to 90% C_2F_6 after three sequential hydrate formation steps [27,28].

Even though the effectiveness of hydrate-based F-gas separation has been proven through the thermodynamic analysis of hydrate formation-dissociation cycles, the dissociation enthalpy (ΔH_d) and hydration numbers of F-gas (CHF_3 or C_2F_6)+N_2 hydrates have never been reported. Hydrate dissociation enthalpy is an inherent thermodynamic property of gas hydrates that is closely related to the energy balance of the hydrate-based gas separation process because hydrate formation is exothermic, whereas hydrate dissociation is endothermic [2]. The hydration number of gas hydrates is useful in estimating the handling capacity of the process because it is based on the fractional occupancy of guest molecules in hydrate cages [2]. Therefore, in this study, the ΔH_d of CHF_3 (20%, 80%, and 100%)+N_2 (balance) hydrates and C_2F_6 (20%, 60%, 80%, and 100%)+N_2 (balance) hydrates were measured using a high-pressure micro-differential scanning calorimeter (HP μ-DSC). The hydration numbers of each hydrate and cage occupancy of the guest mol-

†To whom correspondence should be addressed.
E-mail: ywseo@unist.ac.kr
‡These authors contributed equally to this work and should be considered co-first authors.

ecules were obtained through Rietveld refinement of powder X-ray diffraction (PXRD) patterns for CHF_3 (20%, 80%, and 100%)+N_2 (balance) hydrates and C_2F_6 (20%, 60%, 80%, and 100%)+N_2 (balance) hydrates.

EXPERIMENTAL SECTION

1. Materials and Apparatus

CHF_3 and C_2F_6, each with a purity of 99.999%, were supplied by PSG Gas Co. (Republic of Korea). Gas mixtures of CHF_3 (20% and 80%)+N_2 (balance) and C_2F_6 (20%, 60%, and 80%)+N_2 (balance) were provided by RIGAS Co. (Republic of Korea). Double-distilled, deionized water was used for gas hydrate formation.

Gas hydrates with different F-gas mixtures were formed in a specially designed 316 stainless steel autoclave cell with an internal volume of 250 cm^3 equipped with an impeller-type agitator. This equilibrium cell was immersed in a water-ethylene glycol bath, which was connected to an external circulator (RW-2025G, JEIO Tech, Republic of Korea) with a programmable temperature controller. A resistance temperature detector sensor with a temperature range of 73 K to 1,273 K, which was calibrated using an ASTM 63C thermometer (H-B Instrument Company, USA) with an uncertainty of ±0.03 K, was inserted into the cell to measure the temperature of the inner content. A pressure transducer (S-10, Wika, Germany) with an uncertainty of 0.02 MPa was calibrated using a Heise Bourdon tube pressure gauge (CMM-137219, Ashcroft, USA) and attached to the cell to measure the pressure.

2. PXRD

The crystal structure and cage occupancy of the pure F-gas (CHF_3 or C_2F_6) and F-gas (CHF_3 or C_2F_6)+N_2 hydrates were analyzed using PXRD. The hydrate samples were formed at the desired temperature conditions (at 279.15 K for CHF_3+N_2 gas hydrates and at 275.15 K for C_2F_6+N_2 gas hydrates, with a constant pressure driving force of ΔP=1.0 MPa). The samples were then taken from the cell, immersed in a liquid nitrogen vessel, and ground into fine particles (approximately 50 μm in diameter). The PXRD measurements were performed using a synchrotron monochromatic powder X-ray diffractometer attached to the 6D beamline of the Pohang Accelerator Laboratory (Republic of Korea). The PXRD patterns were collected at 133 K in the range of 2θ=5°-55° and a step size of 0.02°. The precise analysis of the hydrate structures and the cage occupancy of F-gas (CHF_3 or C_2F_6) and N_2 was conducted through Rietveld refinement using the FullProf program.

3. Differential Scanning Calorimetry

The ΔH_d of both pure F-gas (CHF_3 or C_2F_6) and F-gas (CHF_3 or C_2F_6)+N_2 hydrates with different F-gas concentrations was measured using an HP μ-DSC (VII Evo, Setaram Inc., France) equipped with both a sample cell and a reference cell. The sample cell was charged with approximately 20 mg of water and then pressurized with pure F-gas (CHF_3 or C_2F_6) or F-gas (CHF_3 or C_2F_6)+N_2 mixtures at the desired pressure conditions. Multiple cooling-heating cycles were repeated to fully convert initial water to gas hydrates, as shown in Fig. 1(a). When no more residual water was observed, the cell temperature was gradually raised (0.5 K/min) to dissociate the formed gas hydrates. ΔH_d (in J/g water) was initially obtained by integrating the endothermic heat flow curve shown in Fig. 1(b),

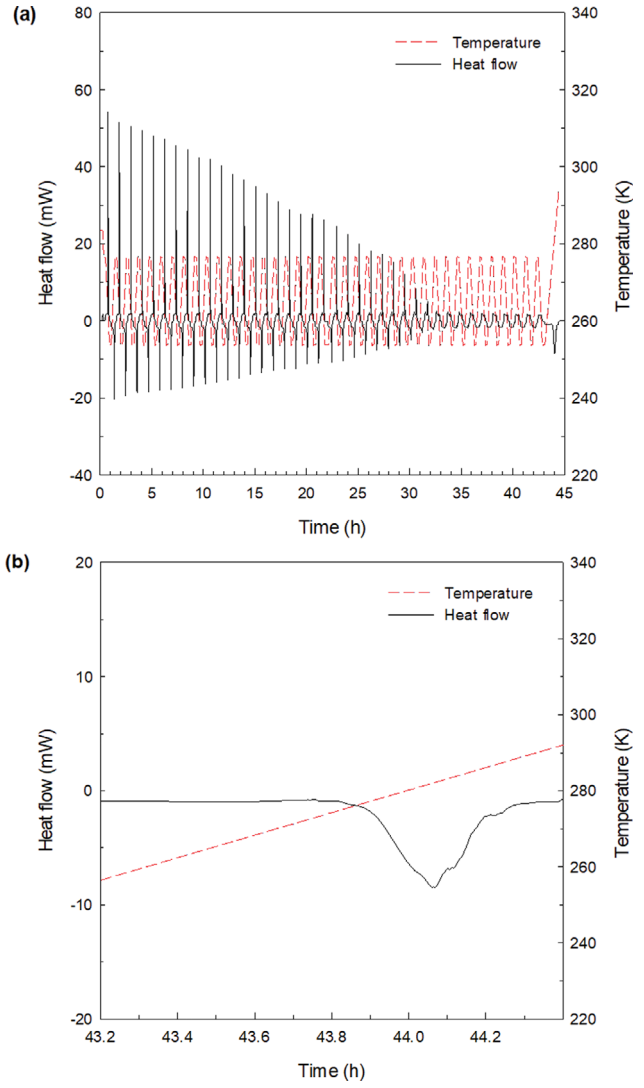

Fig. 1. (a) Heat flow change during the entire cooling-heating cycles for the CHF_3 (20%)+N_2 (80%) hydrate and (b) Heat flow change during the last heating cycle.

and it was then converted into ΔH_d (in kJ/mol gas) by reflecting the hydration number of each gas hydrate. A detailed description of the experimental apparatus and procedure is available in our previous papers [7,8,26-30].

RESULTS AND DISCUSSION

1. PXRD Analysis of Pure F-gas and F-gas+N_2 Hydrates

In this study, the PXRD patterns of pure F-gas (CHF_3 or C_2F_6) and F-gas (CHF_3 or C_2F_6)+N_2 hydrates with various F-gas concentrations (CHF_3: 20% and 80% and C_2F_6: 20%, 60%, and 80%) were collected to confirm the hydrate structure and to reveal the cage occupancy of guest molecules in each hydrate. Figs. 2 and 3 present the PXRD patterns of the pure CHF_3 and CHF_3+N_2 hydrates and the pure C_2F_6 and C_2F_6+N_2 hydrates, respectively. Figs. 2 and 3 clearly demonstrate that both the pure CHF_3 and the CHF_3+N_2 mixtures formed sI hydrates (space group: cubic *Pm-3n*) and that

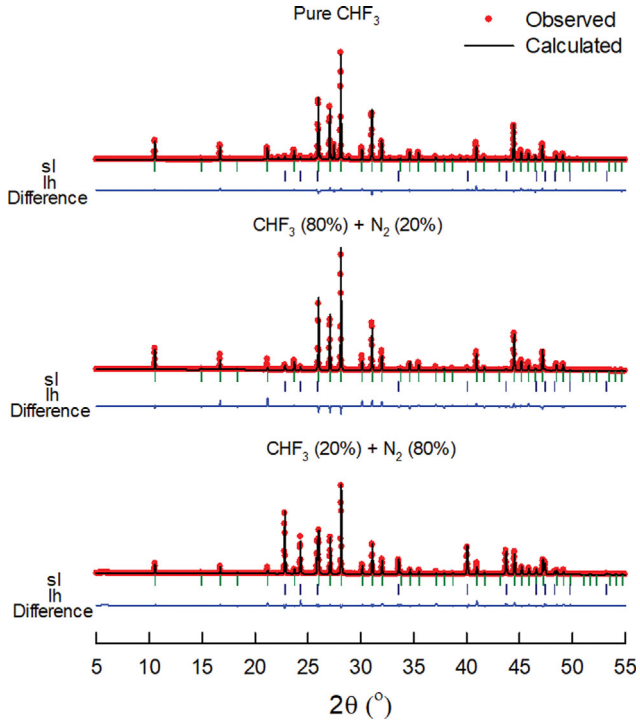

Fig. 2. PXRD patterns of pure CHF_3 and CHF_3+N_2 hydrates.

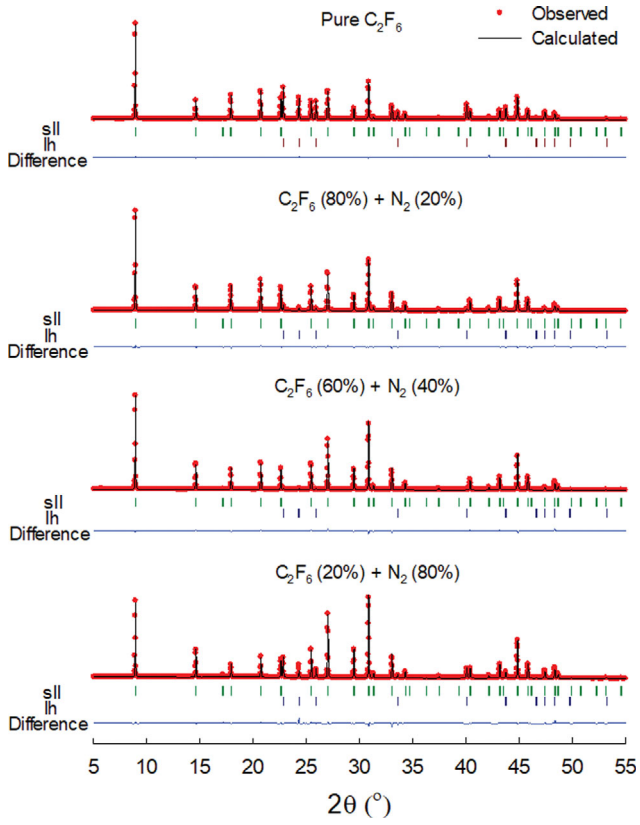

Fig. 3. PXRD patterns of pure C_2F_6 and C_2F_6+N_2 hydrates.

both the pure C_2F_6 and the C_2F_6+N_2 mixtures formed sII hydrates (space group: cubic *Fd-3m*).

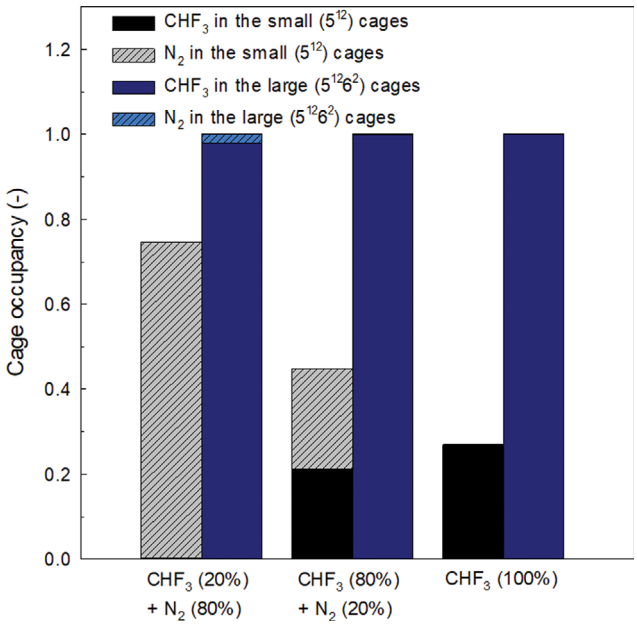

Fig. 4. Cage occupancy of CHF_3 and N_2 in CHF_3+N_2 hydrates.

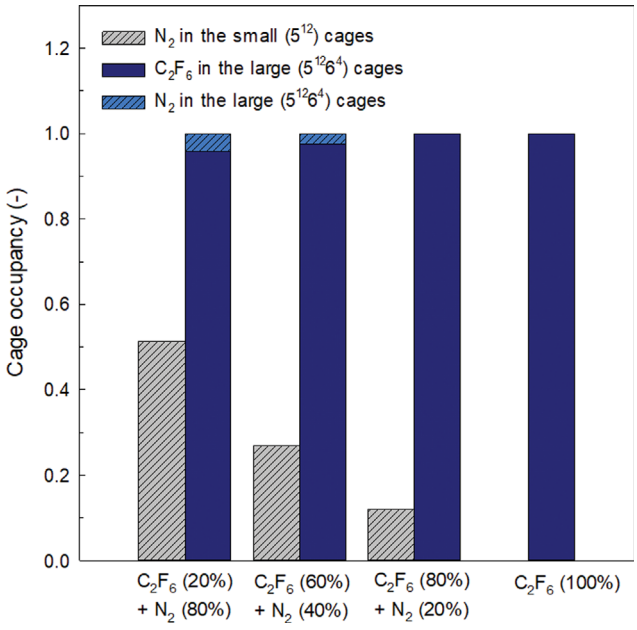

Fig. 5. Cage occupancy of C_2F_6 and N_2 in C_2F_6+N_2 hydrates.

Guest distributions and cage occupancy of guest molecules in the small and large cages of gas hydrates are crucial information because they can be used to elucidate the relative selectivity of guest molecules in the hydrate phase and present the ΔH_d of gas hydrates (ΔH_d in kJ/mol gas) by contributing to the determination of the hydration number. The fractional cage occupancy values of CHF_3 and N_2 molecules in the CHF_3+N_2 hydrates are provided in Fig. 4 and Table 1, and those of C_2F_6 and N_2 molecules in the C_2F_6+N_2 hydrates are presented in Fig. 5 and Table 2. Based on the results reported in our previous study [26], for the pure CHF_3 and C_2F_6 hydrates in this study, CHF_3 and C_2F_6 were reasonably assumed to fully occupy

Table 1. Cage occupancy of CHF_3 and N_2 in pure CHF_3 and CHF_3+N_2 hydrates

Gas mixtures	Occupancy in the small cages (θ_s)		Occupancy in the large cages (θ_L)		Hydration number
	N_2	CHF_3	N_2	CHF_3	
CHF_3 (100%)	-	0.27	-	1	7.0
CHF_3 (80%)+N_2 (20%)	0.2351	0.2131	0.0008	0.9992	6.7
CHF_3 (20%)+N_2 (80%)	0.7426	0.0034	0.0210	0.9790	6.1

Table 2. Cage occupancy of C_2F_6 and N_2 in pure C_2F_6 and C_2F_6+N_2 hydrates

Gas mixtures	Occupancy in the small cages (θ_s)	Occupancy in the large cages (θ_L)		Hydration number
	N_2	N_2	C_2F_6	
C_2F_6 (100%)	-	-	1	17
C_2F_6 (80%)+N_2 (20%)	0.1191	0.0017	0.9983	13.7
C_2F_6 (60%)+N_2 (40%)	0.2689	0.0241	0.9759	11.0
C_2F_6 (20%)+N_2 (80%)	0.5139	0.0425	0.9575	8.4

the large ($5^{12}6^2$) cages of sI and the large ($5^{12}6^4$) cages of sII, respectively. For the CHF_3+N_2 and C_2F_6+N_2 hydrates, both the large cages of sI and sII were assumed to be shared by F-gas (CHF_3 or C_2F_6) and N_2 with full occupancy. As shown in Fig. 4 and Table 1, CHF_3 and N_2 occupied both the large ($5^{12}6^2$) and small (5^{12}) cages of sI hydrates, and the cage occupancy of CHF_3 in the large ($5^{12}6^2$) and small (5^{12}) cages of sI decreased as the N_2 concentration in the feed gas increased. However, in the large cages ($5^{12}6^2$) of sI, CHF_3 had a much larger cage occupancy than N_2 even at N_2-rich gas mixtures such as CHF_3 (20%)+N_2 (80%), which clearly demonstrated that CHF_3 is a more selective hydrate guest than N_2. This high selectivity of CHF_3 accorded with the previous results confirmed by the phase equilibria and pressure-composition diagram of the CHF_3+N_2 hydrate [26]. For the C_2F_6+N_2 hydrates, as shown in Fig. 5 and Table 2, C_2F_6 occupied only the large ($5^{12}6^4$) cages of sII because of its large molecular size, whereas N_2 occupied both the small (5^{12}) and large ($5^{12}6^4$) cages of sII. The large ($5^{12}6^4$) cages of the C_2F_6+N_2 hydrates were predominantly occupied by C_2F_6 molecules, and the cage occupancy of C_2F_6 in the large ($5^{12}6^4$) cages decreased slightly as the N_2 concentration in the feed gas increased. The cage-filling behavior of guest molecules in the C_2F_6+N_2 hydrates clearly demonstrated that C_2F_6 molecules could be captured selectively in the hydrate phase.

In Tables 1 and 2, the hydration number, which was obtained by dividing the number of water molecules in the unit cell of each hydrate structure by the number of guest molecules captured in the hydrate cages, decreased with an increase in the N_2 concentration in the feed gas. This is because the occupancy of N_2 molecules in the hydrate cages, especially in the small (5^{12}) cages, increased with N_2 concentration. This finding indicates that the F-gas (CHF_3 or C_2F_6)+N_2 gas mixtures with higher N_2 concentration require a smaller amount of water for gas hydrate formation.

2. ΔH_d of Pure F-gas and F-gas+N_2 Hydrates

The ΔH_d of gas hydrates is one of the fundamental thermal properties required for designing and operating the hydrate-based gas separation process due to its close relation with heat flow during hydrate formation and dissociation. However, to the best of our knowledge, the ΔH_d values of pure F-gas (CHF_3 or C_2F_6) and F-gas (CHF_3 or C_2F_6)+N_2 hydrates have never been reported in the literature. In this study, the ΔH_d values of pure F-gas (CHF_3 or C_2F_6) and F-gas (CHF_3 or C_2F_6)+N_2 hydrates with various F-gas concentrations (CHF_3: 20% and 80% and C_2F_6: 20%, 60%, and 80%) were experimentally measured using an HP μ-DSC. The ΔH_d (in J/g water) values were initially measured by integrating the endothermic heat flow curves during hydrate dissociation. The ΔH_d (in kJ/mol gas) values were then obtained by combining the ΔH_d (in J/g water) values with the hydration numbers calculated from the cage occupancies of the pure F-gas (CHF_3 or C_2F_6) and F-gas (CHF_3 or C_2F_6)+N_2 hydrates given in Tables 1 and 2. To examine the validity of the experimentally measured ΔH_d values, we compared the ΔH_d values (in kJ/mol gas) of the pure CHF_3 and C_2F_6 hydrates measured using the HP μ-DSC with those of the pure CHF_3 and C_2F_6 hydrates calculated using the Clausius-Clapeyron equation, as well as those of other gas hydrates with the same crystal structure.

The measured and calculated ΔH_d values of the pure CHF_3 hydrate and other gas hydrates with sI are provided in Table 3, and those of the pure C_2F_6 hydrate and other hydrates with sII are presented in Table 4. The measured ΔH_d value (67.6 kJ/mol gas) of CHF_3 hydrate using the HP μ-DSC was in good agreement with the calculated ΔH_d value (68.2 kJ/mol gas) using the Clausius-Clapeyron equation. This measured ΔH_d value was also similar to the ΔH_d values of other sI hydrates, such as CH_4, CO_2, and $CHClF_2$ hydrates. The measured ΔH_d value (127.9 kJ/mol gas) of the C_2F_6 hydrate also matched the calculated one (125.4 kJ/mol gas) and was comparable to the ΔH_d values of other sII hydrates, such as SF_6 and C_3H_8 hydrates. The ΔH_d values of the F-gas+N_2 hydrates with various F-gas concentrations (CHF_3: 20% and 80% and C_2F_6: 20%, 60%, and 80%) are presented in Tables 5 and 6. The ΔH_d values (in kJ/mol gas) of the CHF_3+N_2 hydrates were smaller than that of the pure CHF_3 hydrate and larger than that of the pure N_2 hydrate. They decreased with an increase in N_2 concentration (Table 5). The C_2F_6+N_2 hydrates also exhibited smaller ΔH_d values (in kJ/mol gas) at higher N_2 concentration, and their ΔH_d values (in kJ/

Table 3. ΔH_d of pure CHF_3 hydrate and other sI hydrates

Gas hydrates	ΔH_d (kJ/mol gas)	
CHF_3 hydrate	67.6±0.3	Measured, This work
	68.2	Calculated using the Clausius-Clapeyron equation, This work
CH_4 hydrate	54.2	Measured, Handa [38]
	56.9	Calculated using the Clausius-Clapeyron equation, Sloan and Fleyfel [39]
CO_2 hydrate	57.1±0.2	Measured, Lee et al. [40]
	57.6-63.6	Calculated using the Clapeyron equation, Anderson [41]
$CHClF_2$ hydrate	79.2±1.2	Measured, Mok et al. [42]

Table 4. ΔH_d of pure C_2F_6 hydrate and other sII hydrates

Gas hydrates	ΔH_d (kJ/mol gas)	
C_2F_6 hydrate	127.9±0.4	Measured, This work
	125.4	Calculated using the Clausius-Clapeyron equation, This work
SF_6 hydrate	136.5±2.3	Measured, Ko and Seo [29]
	135.9	Calculated using the Clausius-Clapeyron equation, Ko and Seo [29]
C_3H_8 hydrate	129.2±0.4	Measured, Handa [38]
	126.0	Calculated using the Clausius-Clapeyron equation, Sloan and Fleyfel [39]

Table 5. ΔH_d of CHF_3+N_2 hydrates

Gas mixtures	ΔH_d (J/g water)	ΔH_d (kJ/mol gas)
CHF_3 (100%)	532.1±2.1	67.6±0.3
CHF_3 (80%)+N_2 (20%)	539.5±1.7	64.8±0.2
CHF_3 (20%)+N_2 (80%)	560.0±2.6	62.0±0.3
N_2 (100%)	460.8±1.9 [40]	51.3±0.1 [40]

Table 6. ΔH_d of C_2F_6+N_2 hydrates

Gas mixtures	ΔH_d (J/g water)	ΔH_d (kJ/mol gas)
C_2F_6 (100%)	417.3±0.6	127.9±0.4
C_2F_6 (80%)+N_2 (20%)	446.6±3.5	110.5±0.9
C_2F_6 (60%)+N_2 (40%)	481.6±2.2	95.9±0.4
C_2F_6 (20%)+N_2 (80%)	523.9±5.2	79.2±0.8
N_2 (100%)	460.8±1.9 [40]	51.3±0.1 [40]

mol gas) were smaller than that of the C_2F_6 hydrate and larger than that of the pure N_2 hydrate (Table 6).

ΔH_d is a function of the hydrogen bonds in the hydrate crystal, as well as cage occupation [2]. An increase in N_2 concentration increased N_2 occupancy in the F-gas+N_2 hydrates, which decreased the hydration number and the resulting ΔH_d (in kJ/mol gas). The ΔH_d values of the F-gas+N_2 hydrates were generally closer to that of each pure F-gas hydrate, which indicates that F-gases (CHF_3 or C_2F_6) are more selective in the hydrate phase than N_2.

CONCLUSIONS

This study investigated the guest distribution and ΔH_d of the F-gas (CHF_3 or C_2F_6)+N_2 hydrates. The PXRD patterns demonstrated that the CHF_3 and CHF_3+N_2 hydrates and the C_2F_6 and C_2F_6+N_2 hydrates were sI (*Pm-3n*) and sII (*Fd-3m*), respectively. Through the Rietveld refinement of the PXRD patterns, the cage occupancy of guest molecules in each hydrate cage was quantified. As the N_2 concentration in the feed gas increased, the occupancy of N_2 in the small (5^{12}) cages of sI and sII hydrates increased significantly, which decreased the hydration number of gas hydrates at higher N_2 concentration. The ΔH_d (in kJ/mol gas) values were obtained by combining the ΔH_d (in J/g water) values measured using the HP μ-DSC with the hydration numbers calculated from the cage occupancies of the pure F-gas (CHF_3 or C_2F_6) and F-gas (CHF_3 or C_2F_6)+N_2 hydrates. Since F-gases (CHF_3 or C_2F_6) were more preferentially captured in the hydrate phase than N_2, the ΔH_d values of the F-gas+N_2 hydrates were generally closer to that of each pure F-gas hydrate. The overall experimental results obtained in this study covering the structural and thermodynamic features of the F-gas+N_2 hydrates should be useful for designing and operating the gas hydrate-based F-gas separation process.

ACKNOWLEDGEMENTS

This research was supported by the National Research Foundation of Korea (NRF) (NRF-2021R1A2C2005856 and RS-2022-00144163) and Research Institute of Industrial Science & Technology, Korea (2022H005). This research was also supported by the Carbon Neutral Institute Research Fund (Project # 1.220095.01) of UNIST.

REFERENCES

1. E. D. Sloan, *Nature*, **426**, 353 (2003).
2. E. D. Sloan and C.A . Koh, *Clathrate hydrates of natural gases*, 3rd ed., CRC Press, Boca Raton, FL (2008).
3. J. S. Gudmundsson, M. Parlaktuna and A. A. Khokhar, *SPE Prod.*

Eng., **9**, 69 (1994).
4. T. Sugahara, S. Murayama, S. Hashimoto and K. Ohgaki, *Fluid Phase Equilib.*, **233**, 190 (2005).
5. H. Lu, Y. Tsuji and J. A. Ripmeester, *J. Phys. Chem. B*, **111**, 14163 (2007).
6. T. A. Strobel, C. A. Koh and E. D. Sloan, *Fluid Phase Equilib.*, **261**, 382 (2007).
7. E. Kim, S. Lee, J. D. Lee and Y. Seo, *Chem. Eng. J.*, **267**, 117 (2015).
8. E. Kim, S. Lee, J. D. Lee and Y. Seo, *Fuel*, **164**, 237 (2016).
9. H. D. Nagashima and R. Ohmura, *J. Chem. Thermodyn.*, **102**, 252 (2016).
10. G. Bhattacharjee, V. Barmecha, O. S. Kushwaha and R. Kumar, *J. Chem. Thermodyn.*, **117**, 248 (2018).
11. A. Adeyemo, R. Kumar, P. Linga, J. A. Ripmeester and P. Englezos, *Int. J. Greenhouse Gas Control*, **4**, 478 (2010).
12. A. Eslaminanesh, A. H. Mohammadi, D. Richon, P. Naidoo and D. Ramjugernath, *J. Chem. Thermodyn.*, **46**, 62 (2012).
13. P. Babu, R. Kumar and P. Linga, *Energy*, **50**, 364 (2013).
14. S. Park, S. Lee, Y. Lee, Y. Lee and Y. Seo, *Int. J Greenhouse Gas Control*, **14**, 193 (2013).
15. S. Park, S. Lee, Y. Lee and Y. Seo, *Environ. Sci. Technol.*, **47**, 7571 (2013).
16. Y. Lee, S. Moon, S. Hong, S. Lee and Y. Park, *Chem. Eng. J.*, **389**, 123749 (2020).
17. S. Kim, G. Ko, K. S. Kim and Y. Seo, *J. Chem. Thermodyn.*, **142**, 106024 (2020).
18. R. A. Kini, S. F. Dec and E. D. Sloan, *J. Phys. Chem. A*, **108**, 9550 (2004).
19. T. Maekawa, *Fluid Phase Equilib.*, **243**, 115 (2006).
20. L. J. Rovetto, K. E. Bowler, L. L. Stadterman, S. F. Dec, C. A. Koh and E. D. Sloan, *Fluid Phase Equilib.*, **261**, 407 (2007).
21. S. Lee, Y. Lee, S. Park, Y. Kim, I. Cha and Y. Seo, *J. Chem. Thermodyn.*, **65**, 113 (2013).
22. J. Lee, Y. K. Jin and Y. Seo, *Chem. Eng. J.*, **338**, 572 (2018).
23. J. Lee, K. S. Kim and Y. Seo, *Chem. Eng. J.*, **375**, 121974 (2019).
24. Y. Seo, H. Tajima, A. Yamasaki, S. Takeya, T. Ebinuma and F. Kiyono, *Environ. Sci. Technol.*, **38**, 4635 (2004).
25. I. Cha, S. Lee, J. D. Lee, G. Lee and Y. Seo, *Environ. Sci. Technol.*, **44**, 6117 (2010).
26. E. Kim, E. Shin, G. Ko, S. H. Kim, O. H. Han, S. K. Kwak and Y. Seo, *Chem. Eng. J.*, **306**, 298 (2016).
27. E. Kim, G. Ko and Y. Seo, *ACS Sust. Chem. Eng.*, **5**, 5485 (2017).
28. E. Kim, G. Ko and Y. Seo, *J. Chem. Thermodyn.*, **117**, 43 (2018).
29. G. Ko and Y. Seo, *Environ. Sci. Technol.*, **53**, 12945 (2019).
30. G. Ko and Y. Seo, *Chem. Eng. J.*, **400**, 125973 (2020).
31. W. Choi, Y. Lee, J. Mok, S. Lee, J. D. Lee and Y. Seo, *Chem. Eng. J.*, **358**, 598 (2019).
32. K. Park, S. Y. Hong, J. W. Lee, K. C. Kang, Y. . Lee, M. Ha and J. D. Lee, *Desalination*, **274**, 91 (2011).
33. K. C. Kang, P. Linga, K. Park, S. Choi and J. D. Lee, *Desalination*, **353**, 84 (2014).
34. J. Zhang, M. Yang, Y. Liu, D. Wang and Y. Song, *J. Chem. Thermodyn.*, **104**, 9 (2017).
35. S. Han, Y. W. Rhee and S. P. Kang, *Desalination*, **404**, 132 (2017).
36. M. N. Khan, C. J. Peters and C. A. Koh, *Desalination*, **468**, 114049 (2019).
37. S. D. Seo, S. Y. Hong, A. K. Sum, K. H. Lee, J. D. Lee and B. R. Lee, *Chem. Eng. J.*, **370**, 980 (2019).
38. Y. P. Handa, *J. Chem. Thermodyn.*, **18**, 915 (1986).
39. E. D. Sloan and F. Fleyfel, *Fluid Phase Equilib.*, **76**, 123 (1992).
40. Y. Lee, S. Lee, J. Lee and Y. Seo, *Chem. Eng. J.*, **246**, 20 (2014).
41. G. K. Anderson, *J. Chem. Thermodyn.*, **35**, 1171 (2003).
42. J. Mok, J. Lim, W. Choi, S. Yun, J. Lee, G. Ko and Y. Seo, *Phys. Chem. Chem. Phys.*, **23**, 15693 (2021).